Fast Path and Polarization Manipulation of Telecom Wavelength Single Photons in Lithium Niobate Waveguide Devices

Damien Bonneau,[1] Mirko Lobino,[1] Pisu Jiang,[1] Chandra M. Natarajan,[2] Michael G. Tanner,[2] Robert H. Hadfield,[2] Sanders N. Dorenbos,[3] Val Zwiller,[3] Mark G. Thompson,[1] and Jeremy L. O'Brien[1,*]

[1]*Centre for Quantum Photonics, H. H. Wills Physics Laboratory & Department of Electrical and Electronic Engineering, University of Bristol, Merchant Venturers Building, Woodland Road, Bristol, BS8 1UB, United Kingdom*

[2]*Scottish Universities Physics Alliance and School of Engineering and Physical Sciences, Heriot-Watt University, Edinburgh, EH14 4AS, United Kingdom*

[3]*Kavli Institute of Nanoscience, TU Delft, 2628CJ Delft, The Netherlands*

(Received 26 September 2011; published 31 January 2012)

We demonstrate fast polarization and path control of photons at 1550 nm in lithium niobate waveguide devices using the electro-optic effect. We show heralded single photon state engineering, quantum interference, fast state preparation of two entangled photons, and feedback control of quantum interference. These results point the way to a single platform that will enable the integration of nonlinear single photon sources and fast reconfigurable circuits for future photonic quantum information science and technology.

DOI: 10.1103/PhysRevLett.108.053601 PACS numbers: 42.50.Md, 03.67.Lx

Photons are an appealing approach to quantum information science, which promises enhanced information and communication technologies [1]. An integrated optics approach appears essential for practical applications as well as advances in the fundamental science of quantum optics [2,3]. Progress towards single photon sources [4,5], detectors [6], and circuits that use path [7–11] and polarization [12] encoding have been made, including circuits that are reconfigurable to allow manipulation of photon paths [13,14]. However, these reconfigurable circuits have relied on inherently slow thermal phase shifters and operation at 800 nm. Fast operation of reconfigurable waveguide circuits at telecom wavelengths is crucial for integration with the existing optical telecom networks as well as to benefit from the technologies developed in that area.

Fast routing and manipulation of single photons is essential for both temporally and spatially multiplexed single photon sources [15–18]: quantum communication [19], including device independent quantum key distribution, based on noiseless linear amplifiers [20,21]; circuit [22] and measurement [23–25] based quantum computing [26]; quantum control [27]; and interaction free measurements [28]. Fast control of both path and polarization is crucial for these applications. Proof of principle demonstrations of fast manipulation of single photons have been made using bulk Pockels cells [16,18,25,27,28]; however, there have been no such demonstrations in integrated quantum photonic circuits.

A fast electro-optic effect and the ability to make low loss single mode waveguides at telecom wavelengths using either proton exchange or titanium indiffusion (Ti:LN) makes lithium niobate (LN) an appealing platform for fast reconfigurable quantum photonic devices. Lithium niobate is used in telecommunications applications where 40 GHz modulators are standard; 100 GHz has been demonstrated in the laboratory [29]. Polarization controllers based on the electro-optic effect have also been demonstrated for bright light [30,31]. Lithium niobate is particularly appealing for the prospect of directly integrating periodically poled waveguide photon sources [32].

Fast manipulation of a photon path is possible using the device shown in Fig. 1(b): A Mach-Zehnder interferometer (MZI) fabricated in Ti:LN is composed of two 50:50 directional couplers. Electrodes above each waveguide inside the MZI enable rapid manipulation of the refractive index via the eletro-optic effect. Application of the same positive voltage V to each of the inside electrodes relative to the outside ground electrodes produces an equal and opposite electric field, and hence change in refractive index and phase, in each arm of the MZI.

The same Ti:LN waveguide technology can be used to control the polarization of a single photon when it is integrated with an appropriate electrode architecture [30,31]. The inset to Fig. 1(d) shows a schematic of one stage of the electro-optical polarization controller (PC) used in this work: application of voltages V_1 and V_2 on the electrodes either side of the waveguide, relative to the ground electrode above the waveguide enables an arbitrary electric field vector to be applied perpendicular to the waveguide. The device therefore acts as a tunable wave plate with a controllable thickness ρ and rotation φ that realizes the rotation $\hat{R} = \exp[\frac{2\pi}{\lambda}\rho(\hat{\sigma}_{\mathbf{x}}\sin 2\varphi + \hat{\sigma}_{\mathbf{z}}\cos 2\varphi)]$ where $\hat{\sigma}_x$ and $\hat{\sigma}_z$ refer to the Pauli operators. The PC has 4 identical stages [one is shown in the inset of Fig. 1(d)] which enable the implementation of any unitary operation of the single photon polarization when they are controlled independently.

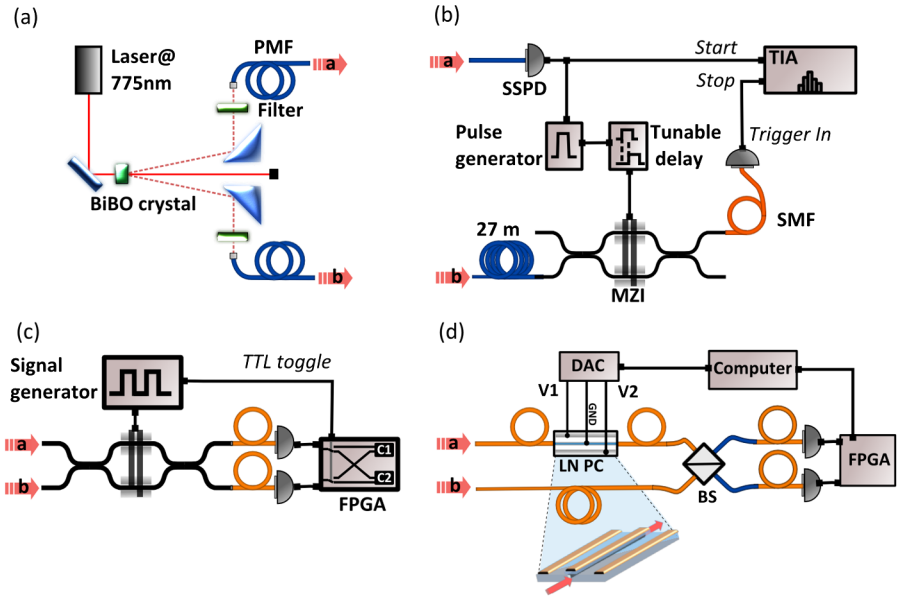

FIG. 1 (color online). Fast path and polarization control of single photons in lithium niobate waveguides. (a) Pulsed spontaneous parametric down-conversion (SPDC) source for photon pairs at 1550 nm. (b) Fast heralded single photon state preparation setup. MZI: lithium niobate Mach-Zehnder interferometer; SSPD: single photon superconducting detectors; SMF: single mode fiber; TIA: time interval analyzer. (c) Fast switching of a two-photon entangled state. The signal generator (SG) drives the MZI with square waves alternating between two voltages $V_0 = -1.6$ V and $V_{\pi/2} = 0.5$ V. Coincidental events for the two voltages are recorded in separate counters embedded in a field programmable gate array (FPGA) board. (d) Fast polarization feedback control of single photons using a lithium niobate polarization controller (PC). The inset shows one stage of the PC consisting of a waveguide surrounded by 3 electrodes.

Photon pairs at 1550 nm wavelength were generated by spontaneous parametric down-conversion (SPDC) in a bismuth borate (BiBO) crystal and collected into two polarization maintaining optical fibers [see Fig. 1(a)], analogous to the ~800 nm SPDC sources that have been used routinely over the last decades. Single photons were detected with two superconducting single photon detectors (SSPDs) [33–36] having system detection efficiencies of 8% and 18%, respectively [37].

Figure 1(b) shows the experimental setup used for heralded single photon state preparation. One photon is measured directly by an SSPD providing the trigger signal for the pulse generator that controlled the MZI. For every trigger event, a voltage pulse was sent to the MZI with a controllable delay. This pulse induced a relative phase shift θ which performed the transformation $|10\rangle \rightarrow \sin\frac{\theta}{2}|10\rangle - \cos\frac{\theta}{2}|01\rangle$. We drove the MZI with a voltage pulse of 20 ns duration and 4 ns rise time that switched between $\theta = \pi$, corresponding to the identity transformation, to $\theta = 0$, for the swap transformation, which routed the photon to the second SSPD. By measuring the number of heralded counts as a function of the delay applied to the driving pulse we reconstructed the time response of the interferometer. Figure 2 shows the number of heralded single photon events as a function of the pulse arrival time, incremented in 0.5 ns steps. The switching efficiency is $97.9 \pm 0.1\%$ with a switching time of 4 ns limited by the waveform of the driving voltage. Travelling-wave electrode designs enable 40 GHz operation in commercial systems and have been used for 100 GHz operation in the laboratory [29].

A continuous range of two-photon states can also be prepared with the reconfigurable MZI: Injecting a pair of photons into its two input ports and applying a voltage V_θ implements the transformation $|11\rangle \rightarrow \frac{\sin\theta}{\sqrt{2}}(|20\rangle - |02\rangle) - \cos\theta|11\rangle$. We verified the tunability of the MZI by continuously changing the voltage from -5 V to $+5$ V and measuring the two photon coincident events at the two output ports. From this measurement we retrieved the $|11\rangle$ component of the prepared states and the associated 2-photon fringe shown in Fig. 3(b), together with the bright light (single photon) fringe [Fig. 3(a)]. The two-photon fringe has a visibility $V_{2\text{ph}} = 95.2 \pm 1.4\%$ and half the period of the single photon fringe. The nonunit visibility is attributed primarily to imperfect spectral overlap of the photons.

Fast two-photon state preparation was realized by applying a 4 MHz square wave that alternates between the voltages V_0 and $V_{\pi/2}$ [see Fig. 1(c)]. With this driving signal the interferometer continuously switches between the output states $|11\rangle$ and $(|20\rangle - |02\rangle)/\sqrt{2}$. Two separate counters $C1$ and $C2$, embedded on the same electronic board, were used to record coincidental events arising from the V_0 and $V_{\pi/2}$ settings, respectively. During this

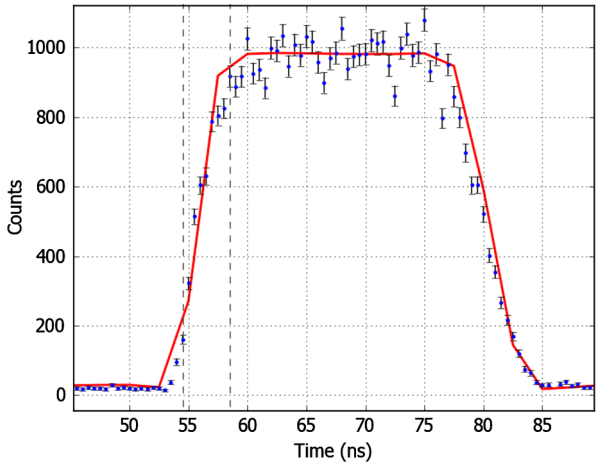

FIG. 2 (color online). Fast path control of single telecom wavelength photons in a lithium niobate Mach-Zehnder interferometer. Number of coincidence events (accumulated in 30 s) as a function of the delay between the optical and the electric pulse [Fig. 1(b)]. The red line is the expected switching behavior computed from the shape of the pulse and the classical characterization of the MZI with a dc voltage. The dots are the measured values. The error bars associated represent the standard deviation for Poissonian statistics.

measurement we varied the relative delay between the two photons by translating one of the two collection fibers of the SPDC source with a motorized stage. As we changed this delay, we recorded two simultaneous count rates for V_0 and $V_{\pi/2}$ as shown in Fig. 4. For V_0 the state $|11\rangle$ is ideally prepared and no dependence of the coincidence count rate on the delay was observed. In contrast, for $V_{\pi/2}$ when we measured the number of coincidences as a function of the relative delay between the two photons we observed the expected Hong-Ou-Mandel interference dip [38] with a visibility $V = 82 \pm 2\%$.

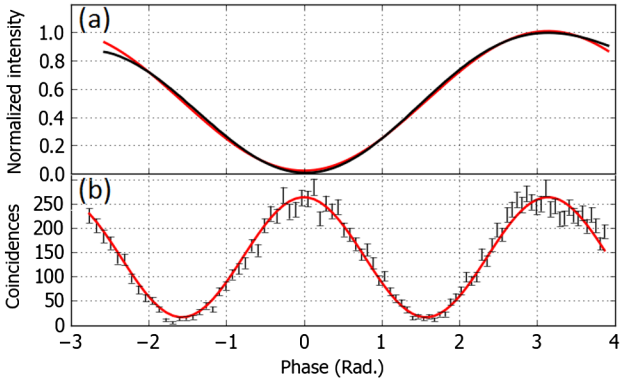

FIG. 3 (color online). Phase control of a two-photon state. (a) Classical interference fringe showing the intensity at one output of the MZI as a function of applied voltage. (b) Two-photon interference fringe showing the number of photon pairs detected simultaneously at each output of the MZI in 40 s. Each dot represents experimental data and the red line is a squared sinusoidal fit. The error bars are $\pm\sigma$ for Poissonian statistics.

The driving electronics of the MZI are understood to be a major contributor to this nonunit visibility since the data shown in Fig. 3(b) with fringe visibility $V_{2\text{ph}} = 95.2 \pm 1.4\%$ corresponds to a Hong-Ou-Mandel interference dip visibility of $V = 91.2 \pm 2.6\%$. The capacitance of the modulator induces a pseudoperiodic voltage oscillation that causes phase oscillations. This effect can be reduced by optimizing the driving electronics.

To control the polarization of single photons we connected the four stages of the PC [Fig. 1(d)] in parallel such that only two driving voltages V_1 and V_2 were required. We used this reconfigurable "integrated wave plate" in an active feedback loop implemented to maximize the polarization indistinguishability between two single photons interfering at a 50/50 beam splitter (BS) [Fig. 1(d)]. Assuming that the state of the photons arriving at the BS is $|\psi\rangle_1 \otimes |\phi\rangle_2 = (\cos\alpha|H\rangle_1 + e^{i\beta}\sin\alpha|V\rangle_1) \otimes (\cos\gamma|H\rangle_2 + e^{i\delta}\sin\gamma|V\rangle_2)$ and that the polarization drift of the photons is slow compared to the time required to complete a full feedback loop, it is possible to align their polarization by implementing the transformation $\hat{R}$ satisfying $\hat{R}|\psi\rangle_1 = |\phi\rangle_2$ with our integrated PC.

Figure 1(d) shows the experimental setup: here the photons from the SPDC source were collected into two single mode optical fibers that were not polarization maintaining. One photon was sent through the polarization controller and the other through a fiber patch cord to arrive simultaneously at the beam splitter. We first characterized the PC by fixing the two collection fibers to the table and measuring the number of coincidences from the two outputs of the BS as a function of V_1 and V_2. Figure 5(a) shows

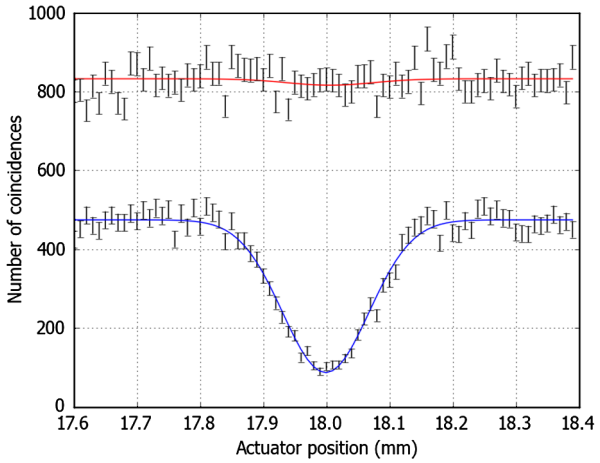

FIG. 4 (color online). Fast switching of a two-photon state. By delaying the arrival time of one photon with respect to the other (shown on the x axis), we simultaneously record the coincidental counts integrated over 210 s (y axis) for each voltage applied to the MZI. In the case where the applied voltage is close to $V_{\pi/2} = 0.5$ V, the MZI acts as a balanced beam splitter, quantum interference occurs and a dip of $82 \pm 2\%$ visibility is recorded. For $V_0 = -1.6$ V, the MZI acts as a crosser, therefore, the photons do not interfere and a visibility of $2 \pm 3\%$ is recorded.

the measured coincidence pattern with a visibility of the quantum interference $V_{\mathrm{pol}} = 87 \pm 1\%$. Maximum coincidental event detection was observed when the two photon polarizations were orthogonal while low coincidental detection corresponded to identical polarization; nonunit visibility is mainly due to multiphoton events that arise from a higher pump power of 400 mW (95% visibility was observed in a conventional Hong-Ou-Mandel experiment at the 10 mW power used for all other 2-photon demonstrations reported here).

Next we used the polarization controller to automatically optimize the quantum interference between two single photons which were nominally identical in all degrees of freedom except for polarization. For this task there is no need to perform tomography of any of the states since any minimum in the number of coincidences is the global minimum [37]. Because of this property of the coincidence function we implemented a feedback loop based on the gradient descent method. Figure 5(b) shows the convergence of six coincidence paths towards the minimum, starting from six different random polarizations. In all cases the system evolves towards the point where the number of coincidences is minimum which implies maximum indistinguishability between the photons.

The dynamic response of the feedback loop was measured by periodically changing the polarization of one photon via the rotation of a computer controlled (bulk) half wave plate placed before the collection fiber of the SPDC source. This setup simulates the situation where a single photon propagating in a controlled environment interferes with a second photon coming from a noisy channel. In this situation the PC is used to compensate for polarization fluctuation of the second photon and restore maximum indistinguishability. The overlap between the polarizations of the two photons is restored after ~4 iterations [Fig. 5(c)]. Although our polarization controller in principle allows operation of the feedback loop at MHz rates, in our current demonstration we chose an integration time of 2 s per polarization setting, as our coincidence count rate was ~100 Hz. It is worth mentioning that possible dc drift of the device may happen on the scale of several hours [39] but it is automatically compensated by the feedback loop.

Rapid manipulation of the polarization and path degrees of freedom of single photons will be essential for future quantum technologies as well as fundamental quantum science. The ability to perform both path and polarization manipulation in a single platform is particularly appealing. Furthermore, lithium niobate promises the ability to directly integrate periodically poled LN single photon sources. Ultimately it should also be possible to integrate SSPDs into the waveguide circuit via growth of NbTiN directly onto LN substrates [35]. A particularly important future application is multiplexed single photon sources [15–18]: The setup shown in Figs. 1(a) and 1(b) represents a single unit of such a source: by removing the pump beam block and replicating the BiBO crystal and MZI N times, simple switching logic would enable a near-deterministic single photon source to be realised, provided efficiencies and losses could be controlled; a fully integrated architecture will help reduce such losses. The state-of-the-art modulation speed available (40 GHz) exceeds the speed of the digital electronic, working in the 1 GHz regime, required to perform coincidental detections and apply feedback in a reconfigurable circuit. Finally we note that the heralding efficiency reported here is not state of the art

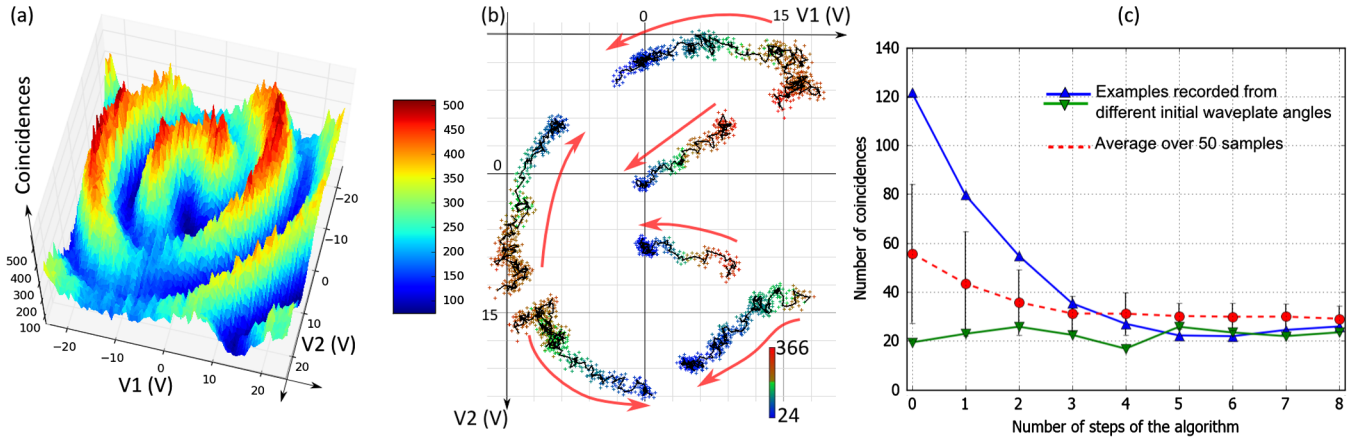

FIG. 5 (color online). Polarization control of 1550 nm photons, using the device and setup shown in Fig. 1(c). (a) Coincident photon counts in 4 s as a function of applied voltages V_1 and V_2. (b) Paths generated by applying the feedback loop algorithm starting from a random V_1 and V_2. Colored points represent the measurement of the number of coincidences integrated over 4 s while black lines show the path followed by the algorithm. The arrows indicate the direction of the evolution for the six different initial conditions. (c) Dynamic of the feedback loop, showing the number of coincidences as a function of the number of steps of the algorithm. The blue and green lines are two examples recorded from different initial wave plate angles. The dashed line is the average of 50 random samples.

due to coupling losses from the MZI to the SSPDs. This could be significantly improved by using waveguide based SSPDs [40,41], integrated directly with the waveguide circuits presented in this Letter.

Reconfigurable circuits with path and polarization encoding will find applications across photonic quantum information science and technology ranging from quantum communication, quantum control, quantum measurement and quantum information processing.

We thank O. Alibart and S. Tanzilli for useful discussions. This work was supported by Nokia, EPSRC, ERC, PHORBITECH, QUANTIP, NSQI, FOM, and NWO (Vidi grant). M. L. acknowledges a Marie Curie IIF. R. H. H. acknowledges a Royal Society University Research Fellowship. J. L. O'B. acknowledges a Royal Society Wolfson Merit Award.

*Jeremy.OBrien@bristol.ac.uk

[1] J. L. O'Brien, A. Furusawa, J. Vučković, Nature Photon. **3**, 687 (2009).
[2] A. Politi, J. C. F. Matthews, M. G. Thompson, and J. L. O'Brien, IEEE J. Sel. Top. Quantum Electron. **15**, 1673 (2009).
[3] Jeremy O'Brien, Brian Patton, Masahide Sasaki, and Jelena Vuckovic, Special issue on Integrated Quantum Optics, [New J. Phys. **13** (2011)].
[4] Philippe Grangier, Barry Sanders, and Jelena Vuckovic, Special issue on Single Photons on Demand, [New J. Phys. **6** (2004)].
[5] A. J. Shields, Nature Photon. **1**, 215 (2007).
[6] R. H. Hadfield, Nature Photon. **3**, 696 (2009).
[7] A. Politi *et al.*, Science **320**, 646 (2008).
[8] A. Politi, J. C. F. Matthews, and J. L. O'Brien, Science **325**, 1221 (2009).
[9] A. Peruzzo *et al.*, Science **329**, 1500 (2010).
[10] A. Peruzzo *et al.*, Nature Commun. **2**, 224 (2011).
[11] A. Laing *et al.*, Appl. Phys. Lett. **97**, 211109 (2010).
[12] L. Sansoni *et al.*, Phys. Rev. Lett. **105**, 200503 (2010).
[13] J. C. F. Matthews, A. Politi, A. Stefanov, and J. L. O'Brien, Nature Photon. **3**, 346 (2009).
[14] B. J. Smith *et al.*, Opt. Express **17**, 13 516 (2009).
[15] A. L. Migdall, D. Branning, and S. Castelletto, Phys. Rev. A **66**, 053805 (2002).
[16] X. S. Ma *et al.*, Phys. Rev. A **83**, 043814 (2011).
[17] T. Jennewein, M. Barbieri, and A. G. White, J. Mod. Opt. **58**, 276 (2011).
[18] K. T. McCusker and P. G. Kwiat, Phys. Rev. Lett. **103**, 163602 (2009).
[19] N. Gisin, G. Ribordy, W. Tittel, and H. Zbinden, Rev. Mod. Phys. **74**, 145 (2002).
[20] G. Y. Xiang *et al.*, Nature Photon. **4**, 316 (2010).
[21] F. Ferreyrol *et al.*, Phys. Rev. Lett. **104**, 123603 (2010).
[22] E. Knill, R. Laflamme, and G. J. Milburn, Nature (London) **409**, 46 (2001).
[23] M. A. Nielsen, Phys. Rev. Lett. **93**, 040503 (2004).
[24] D. E. Browne and T. Rudolph, Phys. Rev. Lett. **95**, 010501 (2005).
[25] R. Prevedel *et al.*, Nature (London) **445**, 65 (2007).
[26] J. L. O'Brien, Science **318**, 1567 (2007).
[27] G. G. Gillett *et al.*, Phys. Rev. Lett. **104**, 080503 (2010).
[28] P. G. Kwiat *et al.*, Phys. Rev. Lett. **74**, 4763 (1995).
[29] A. Kanno *et al.*, IEICE Electron. Expr. **7**, 817 (2010).
[30] A. J. P. van Haasteren, J. J. G. M. van der Tol, M. O. van Deventer, and H. J. Frankena, J. Lightwave Technol. **11**, 1151 (1993).
[31] N. G. Walker and G. R. Walker, J. Lightwave Technol. **8**, 438 (1990).
[32] A. Martin *et al.*, New J. Phys. **12**, 103005 (2010).
[33] R. H. Hadfield *et al.*, Opt. Express **13**, 10 846 (2005).
[34] C. M. Natarajan *et al.*, Appl. Phys. Lett. **96**, 211101 (2010).
[35] S. N. Dorenbos *et al.*, Appl. Phys. Lett. **93**, 131101 (2008).
[36] M. G. Tanner *et al.*, Appl. Phys. Lett. **96**, 221109 (2010).
[37] See Supplemental Material at http://link.aps.org/supplemental/10.1103/PhysRevLett.108.053601 for details on the single photon source, the interference of photons with arbitrary polarization, and the superconducting single photon detectors.
[38] C. K. Hong, Z. Y. Ou, and L. Mandel, Phys. Rev. Lett. **59**, 2044 (1987).
[39] A. Chen, R. W. Smith, and W. E. Derbyshire, *Lasers and Electro-Optics Society, 2002. LEOS 2002. The 15th Annual Meeting of the IEEE* Vol. 2 (IEEE, New York, 2002), p. 885.
[40] W. Pernice *et al.*, arXiv:1108.5299.
[41] J. P. Sprengers *et al.*, Appl. Phys. Lett. **99**, 181110 (2011).